Tomas Bata University in Zlín
Library

Tuning the conductivity, morphology, and capacitance with enhanced antibacterial properties of polypyrrole by acriflavine hydrochloride

Citation

GUPTA, Sonal, Udit ACHARYA, Hana PIŠTĚKOVÁ, Oumayma TABOUBI, Zuzana MORÁVKOVÁ, Martina KAŠPAROVÁ, Petr HUMPOLÍČEK, and Patrycja BOBER. Tuning the conductivity, morphology, and capacitance with enhanced antibacterial properties of polypyrrole by acriflavine hydrochloride. *ACS Applied Polymer Materials* [online]. vol. 3, iss. 12, American Chemical Society, 2021, p. 6063 - 6069 [cit. 2023-04-17]. ISSN 2637-6105. Available at https://pubs.acs.org/doi/10.1021/acsapm.1c00775

DOI

https://doi.org/10.1021/acsapm.1c00775

Permanent link

https://publikace.k.utb.cz/handle/10563/1010671

This document is the Accepted Manuscipt version of the article that can be shared via institutional repository.

TBU Publications
Repository of TBU Publications
publikace.k.utb.cz

Tuning the Conductivity, Morphology, and Capacitance with Enhanced Antibacterial Properties of Polypyrrole by Acriflavine Hydrochloride

Sonal Gupta, Udit Acharya, Hana Pištěková, Oumayma Taboubi, Zuzana Morávková, Martina Kašparová, Petr Humpolíček, and Patrycja Bober*

Sonal Gupta - Institute of Macromolecular Chemistry, Czech Academy of Sciences, 162 06 Prague 6, Czech Republic
Udit Acharya - Institute of Macromolecular Chemistry, Czech Academy of Sciences, 162 06 Prague 6, Czech Republic
Hana Pištěková - Centre of Polymer Systems, Tomas Bata University in Zlín, 760 01 Zlín, Czech Republic
Oumayma Taboubi - Institute of Macromolecular Chemistry, Czech Academy of Sciences, 162 06 Prague 6, Czech Republic
Zuzana Morávková - Institute of Macromolecular Chemistry, Czech Academy of Sciences, 162 06 Prague 6, Czech Republic;®orcid.org/0000-0001-8128-1040
Martina Kašparová - Centre of Polymer Systems, Tomas Bata University in Zlín, 760 01 Zlín, Czech Republic
Petr Humpolíček - Centre of Polymer Systems and Faculty of Technology, Tomas Bata University in Zlín, 760 01 Zlín, Czech Republic; ® orcid.org/0000-0002-6837-6878

ABSTRACT: In this study, a simple one-step preparation of polypyrrole (PPy) assisted by an organic dye, acriflavine hydrochloride (AF), was investigated. The presence of a dye resulted in the development of PPy nanofibers with the conductivity enhanced up to 14 S cm^{-1}. The structural analysis by Fourier-transform infrared and Raman spectroscopies confirmed the interaction of the AF with PPy. As far as the electrochemical activity of PPy is concerned, the gravimetric capacitance increased up to 85 F g^{-1} with the help of a AF. Additionally, a substantial improvement in the antibacterial activity against *Staphylococcus aureus* and *Escherichia coli* bacteria for all the PPy-containing organic dye was achieved. The conductivity, morphology, capacitance, and remarkable antibacterial properties of PPy tuned by an organic dye enable applications wherever the electroconductivity and antibacterial activity should meet requirements, for example, wound healing, electrochemical sensors, bioactuators, or even regenerativ medicine.

KEYWORDS: *acriflavine hydrochloride, polypyrrole, nanofibers, conductivity, capacitance, antibacterial activity*

1. INTRODUCTION

Considerable progress has been made in the field of conducting polymers due to their versatile applications, particularly in biosensors, electrochemical capacitors, and for employment in biomedical and health care sectors.[1,2] The cost-effective, easy synthesis, environmental stability, and tunable properties such as conductivity and morphology of polypyrrole (PPy), in addition to its biocompatibility, make it a high-ranking conducting polymer.[3] The combination of antibacterial properties and conductivity can be successfully utilized in various application fields, for example, in smart wearable equipment, where conductivity can be used for heating or sensing and antibacterial

properties add to sustainable use.[4] Marakova et al. have demonstrated the enhanced antibacterial effect of PPy-embedded cotton along with lower cytotoxicity and further studied the effect of silver nanoparticles on the conductivity and antibacterial activity of PPy.[5] Liu et al. have successfully synthesized PPy-AgCl nanocomposites in the presence of methyl orange and obtained a conductivity of 17 S cm^{-1} with enhanced antibacterial properties.[6]

Efforts to improve the antimicrobial properties of PPy with the use of biopolymers such as cellulose,[7] dextrin,[8] chitosan,[9]and gelatin[10] have been made. Also, metals or metal oxides have been used for the preparation of PPy composites to achieve promising antibacterial properties; however, their high cost limits applications in biomedicine.[11-15] Moreover, abundant research work shows that high conductivity of PPy can be accomplished by introducing carbon nanotubes,[16] graphene,[17] or graphene oxide[18] in addition to its desirable capacitive properties.[19,20] Besides these, PPy with the cost-effective organic dyes have recently attracted interest of researchers for the high conductivity and easy tuning of morphology in the resulting composites.

In previous studies, our group has demonstrated the significance of various dyes such as methyl orange, ethyl orange, safranin and methyl red in improving the conductivity of PPy. Additionally, we successfully gained controlled morphology of PPy such as nanorods, nanotubes, nanofibers, and so forth.[21-23] One of the recent studies has presented the cytotoxic activity of biocompatible PPy prepared in the presence of acid blue [25], signifying its potential biomedical applications.[24] However, regarding its antibacterial assessments, surprisingly, nothing is known, which thus encouraged our current research work.

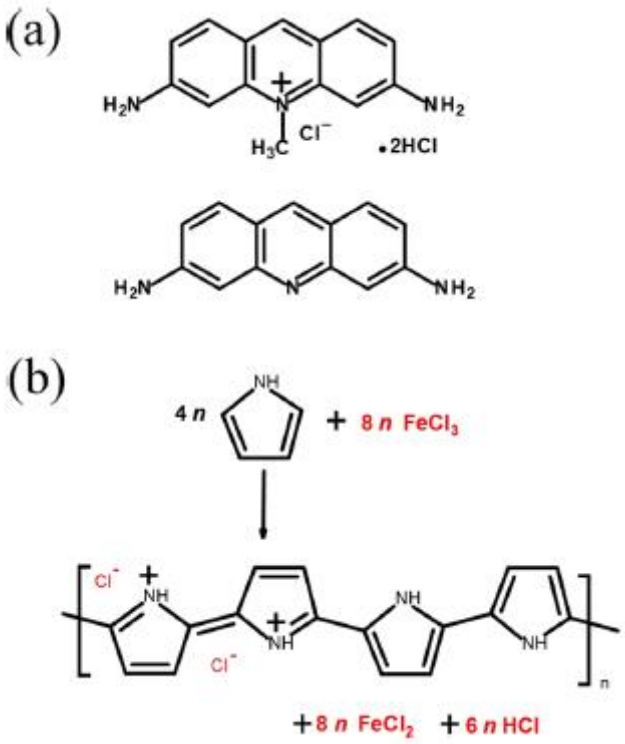

Figure 1. (a) Synthesis of PPy using iron(III) chloride as an oxidant and (b) structure of AF.

The present study reports the effect of an organic dye, acriflavine hydrochloride (AF) (**Figure 1a**), not only on electrical conductivity and morphology but also on the electrochemical activity of PPy. The

high capacitive behavior displayed by nanofibers compared to pristine globular PPy is also discussed. AF is well known for its antiseptic properties and ability to treat bacterial and fungal infections as well as is used in different biomedical applications.[25,26] For this purpose, the utmost emphasis has been made in investigating the antibacterial activity of conducting PPy prepared in the presence of AF. The enhanced capacitance of the conducting nanofibrous PPy with optimistic antibacterial activity is presented in this work.

2. EXPERIMENTAL SECTION

2.1. *Chemicals and Reagents*. Pyrrole (98%), iron(III) chloride hexahydrate, AF (mixture of 3'6-diamino-10-methylacridinium and 3'6-diaminoacridine)' and Nafion 117 solution (lower aliphatic alcohols and water mixture) supplied from Sigma-Aldrich were employed without any further purification.

2.2. Preparation of PPy with or without the AF Dye. PPywas prepared by the oxidation of 0.15 M pyrrole using 0.3 M iron(III) chloride as an oxidant (**Figure 1b**). Both pyrrole and $FeCl_3 \cdot 6H_2O$ were dissolved separately in 50 mL of distilled water. Then, the reaction was started by fast mixing of the two solutions followed by vigorous shaking (1-2 min). The resultant 100 mL reaction mixture contained a fixed molar ratio of the oxidant to monomer, that is, [oxidant]/[pyrrole] = 2. Then, the polymerization was carried out by leaving the reaction mixture undisturbed overnight at room temperature. The obtained product was filtered and washed with excess of 0.2 M HCl and ethanol, and the black solid, PPy, was dried in a desiccator over silica gel to a constant weight. For the synthesis of PPy in the presence of a AF, a sequence of AF concentrations from 2.5 to 10 mM was selected. The dye was dissolved in 50 mL of distilled water along with pyrrole. The next step involved the addition of an oxidant to the solution of the monomer with the dye, and the reaction proceeded in a similar way as described above.

2.3. Characterization. The morphology of the PPy samples was examined with an MAIA3 TESCAN scanning electron microscope and TEC-NAI G2 SPIRIT transmission electron microscope.

DC conductivity was measured at room temperature by a van der Pauw method with spring-loaded electrodes on compressed pellets (diameter 13 mm, thickness 1.0 ± 0.3 mm) prepared under 530 MPa pressure using a hydraulic press TRYSTOM H-62 (Czech Republic). A Keithley 230 programmable voltage source in serial connection with a Keithley 196 System DMM was used as the current source, and the potential difference was measured with a Keithley 181 nanovoltmeter. The values were determined as an average from the measurements in two perpendicular directions taken from the linear part of the current—voltage curve.

Fourier-transform infrared (FTIR) spectra of the powders dispersed in potassium bromide pellets were registered using a Thermo Nicolet NEXUS 870 FTIR spectrometer with a DTGS TEC detector in the 400—4000 cm^{-1} wavenumber region.

Raman spectra were recorded on a Renishaw InVia Reflex Raman microspectrometer. The spectra were excited with HeNe 633 nm. A research-grade Leica DM LM microscope was used to focus the laser beam. The scattered light was analyzed with a spectrograph using holographic gratings of 1800 lines mm^{-1}. A Peltier-cooled charge-coupled device detector (576 X 384 pixels) registered the dispersed light.

Thermogravimetric analysis (TGA) of the PPy sample was performed on a PerkinElmer Pyris 1 thermogravimetric analyzer in a temperature range 35—800 °C at a rate of 10 °C min^{-1} with a fixed air flow rate at 25 mL min^{-1}.

Electrochemical studies were performed on a Metrohm AUTOLAB PGSTAT302N potentiostat in a three-electrode cell. Glassy carbon (diameter = 3 mm), Ag/Ag^+ wire, and Pt wire were used as the working, pseudoreference, and counter electrodes, respectively. As a supporting electrolyte, 0.2 M HCl was used. For each sample preparation, ~5 mg of ground PPy with or without the dye was uniformly dispersed in 1 mL of a mixture containing 590 µL of Milli-Q water, 400 µL of isopropanol, and 10 µL of Nafion. Each measurement was carried out by drop-casting 1 µL of the dispersion onto a glassy carbon electrode under an inert atmosphere.

The gravimetric capacitance was calculated from the cyclic voltammograms (CVs) using the following equation

$$C = \frac{\int_{V_1}^{V_2} I \, dV}{2mv\Delta V}$$

where $\int I dV$ depicts the area under the CV, m (g) represents the mass of the active material drop-casted, v (V/s) is the scan rate, and ΔV is the potential window from V_1 to V_2.

For antibacterial testing, each sample was ground in a porcelain mortar to a fine powder and then weighed to prepare a stock concentrated suspension. From each sample, the stock concentrated suspension was prepared in sterile Mueller-Hinton broth (MHB) medium at a concentration of 64 mg mL^{-1}, and the stock suspension was further diluted to concentrations of 32, 16, 8, 4, 2, 1, 0.5, 0.25, 0.12, 0.062, and 0.031 mg mL^{-1}.[27] An equal amount of the bacterial suspension (inoculum) in MHB was added to each concentration, and after thorough homogenization, the tubes were incubated for 24 h at 35 °C. Then, 0.1 mL was taken from each tube and spread on the surface of tryptone soya agar (in duplicate for each concentration). After incubation at 35 °C for 18-24 h, the growth of the test bacteria on the surface of the plates was evaluated and the minimum inhibitory concentration (MIC) was determined accordingly. The tests were performed with Gram-positive *Staphylococcus aureus (S. aureus)* CCM 4516 (inoculum concentration 2.2 X 10^6 cfu mL^{-1}) and Gramnegative *Escherichia coli (E. coli)* CCM 4517 (inoculum concentration 8.4 X 10^5 cfu mL^{-1}). The experimental setup was performed according to the procedure described in Nature Protocols.[27]

3. RESULTS AND DISCUSSION

3.1. Morphology. In general, pristine PPy shows a globular morphology which could be tuned to nanorods, nanotubes, nanofibers, or irregular patterns upon addition of organic dyes such as safranin, methyl orange, acid blue 25, or methyl red, respectively, to the polymerization mixture.[21-24] Herein, the conversion from globular PPy (**Figures 2a and 3a**) to nanofibers (**Figures 2b and 3b**) can be seen clearly upon introduction of even a small quantity of the AF dye. Upon increasing the dye concentration to 7.5 mM, PPy nanofibers show enlarged dimensions, signifying the role of concentration of the dye in determining the morphology (**Figures 2c and 3c**). However, the nanofibrous morphology of PPy is maintained even for the highest concentration of the dye, that is, 10 mM (excess of the dye in the polymerization mixture). The aggregate formation of undefined shape can also be noticed for this dye concentration (**Figures 2d and 3d**).

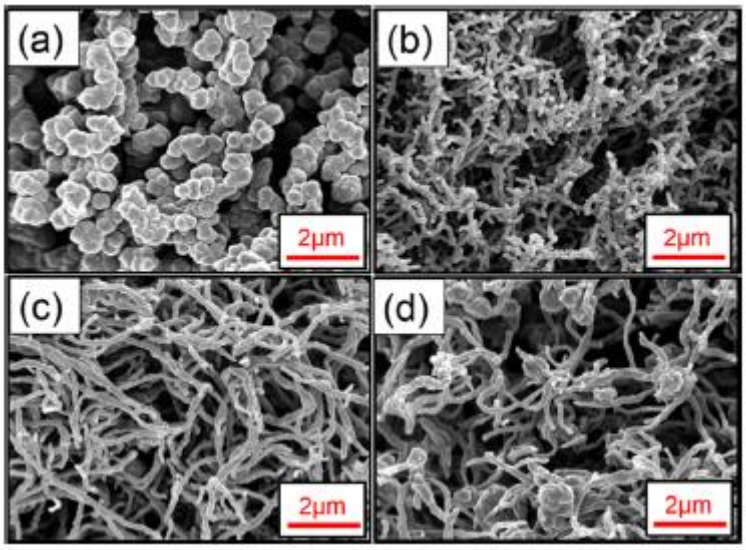

Figure 2. SEM micrographs of PPy prepared in the presence of (a) 0, (b) 2.5, (c) 7.5, and (d) 10 mM of AF.

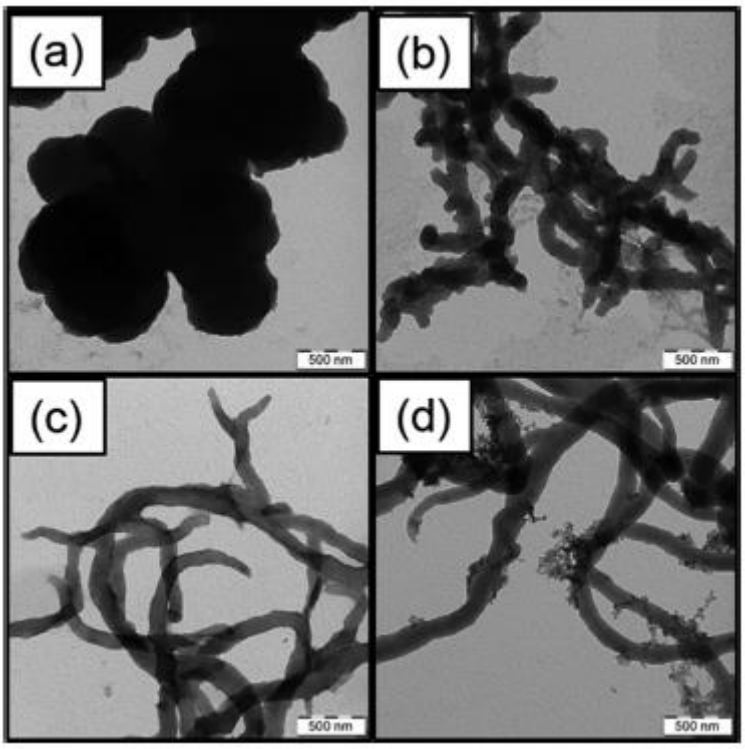

Figure 3. TEM micrographs of PPy prepared in the presence of (a) 0, (b) 2.5, (c) 7.5, and (d) 10 mM of AF.

3.2. FTIR Spectra. Infrared spectra of the pristine PPy, AF dye, and PPy with various concentrations of the AF dye are displayed in **Figure 4**. In the spectrum of the AF dye, the band corresponding to the N-H+ stretching vibration of amine hydrochloride (—NH_3^+) is observed at 3303 cm^{-1}. The C=C stretching vibrations in the aromatic ring show absorptions at 1597 cm^{-1}.

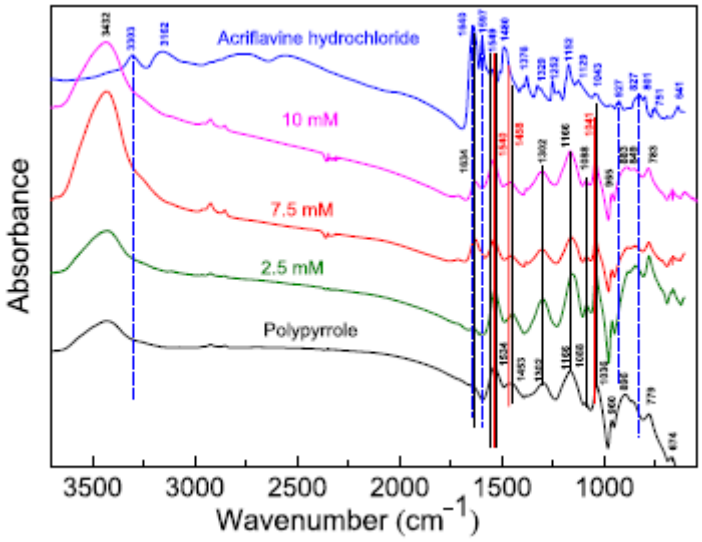

Figure 4. FTIR spectra of pristine PPy, acriflavine dye, and PPy prepared at various concentrations of AF. The peaks referring to AF are marked with dashed blue lines, PPy with black solid lines, and the peak shifts with red solid lines.

In addition, the peak at 1480 cm-1 refers to the ring stretching vibration of the phenazine ring. The range, 1200-1400 cm^{-1}, represents the C—N stretching modes.28 The peaks at 927 and 827 cm^{-1} represent out-of-plane C-H deformation on a trisubstituted aromatic ring structure present in the phenazine ring.

The spectra of PPy prepared in the presence of the dye reveal the main characteristic bands of PPy and a small shoulder at 1597 cm^{-1} that corresponds to the aromatic ring vibrations of AF. A weak absorption band is also observed at about 1634 cm^{-1} and can be related to AF ring-stretching vibrations (observed exactly at 1640 cm-1 in pure AF) or to the presence of the carbonyl group due to the nucleophilic attack of water during the polymerization.[29] The latter would indicate strong overoxidation of the sample induced by AF presence. The band observed at 1534 cm^{-1} (C-C stretching vibrations in the pyrrole ring) of the pristine PPy shifts to 1540 cm^{-1} after adding 10 mM of AF. The band of C-N stretching vibrations located at 1453 cm^{-1} shifts to 1458 cm^{-1}. The broad band at 1302 cm^{-1} corresponding to the C-H or C-N inplane deformation vibration remains at the same position as well as the peak at 1166 cm^{-1} which refers to the C-H inplane deformation vibration. The peak at 1036 cm^{-1} representing C-H out-of-plane bending shifts to 1041 cm^{-1} upon addition of AF. The small peak at 1597 cm^{-1} that appears in the spectra of PPy with various concentrations of the dye in addition to the peak shifts confirms the presence of the AF dye and its interaction with PPy. All mentioned shifts are in the direction to higher wavenumbers, indicating a slight stiffening of the pyrrole ring, most likely due to π-π interactions with AF.

3.3. Raman Spectra. Raman spectra collected with a laser excitation wavelength of 633 nm as presented in **Figure 5** provide information on the charge distribution on the PPy chains since both polarons and bipolarons are resonantly enhanced with this excitation line. On the other hand, the AF dye is out of resonance with this excitation wavelength and thus is not observed.

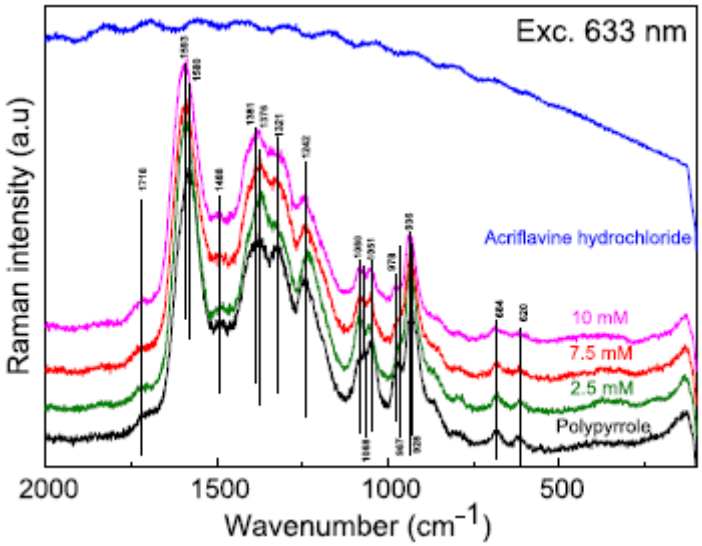

Figure 5. Raman spectra (excitation line 633 nm) of AF and PPy in the absence and presence of various concentrations of the AF.

In the recorded spectrum of pristine PPy, the typical band related to the backbone stretching of C=C bonds and the inter-ring C—C in the backbone of the polaron structure is located at 1580 cm^{-1}.[30—32] The band of C—N stretching vibrations in the pyrrole ring is located at 1488 cm^{-1}.[29,30] The doublet situated at 1376 and 1321 cm^{-1} corresponds to the ring stretching vibrations of PPy. The band located at higher wavenumbers is assigned to the vibrations of charged PPy, and the second one refers to the C—C ring stretching of neutral units.[30-32] The band maximum at about 1242 cm^{-1} is assigned to the C-H antisymmetric in-plane bending vibrations.29,33 In the region 1090-1050 cm^{-1}, two peaks are detected: 1068 cm^{-1} is attributed to the C-H in-plane deformation vibrations of protonated species and 1051 cm^{-1} corresponds to the C-H in-plane deformations in the neutral units.[30,32,34] The bands at 967 and 928 cm^{-1} are assigned to the in-plane ring deformation related to the polaron and bipolaron states of PPy, respectively.[30,31,35] The small shoulder at 1718 cm^{-1}, observed in all samples, is connected to the carbonyl groups and overoxidation.

In the spectra of PPy in the presence of AF, we observe the same bands with blue shifts in comparison to the spectrum of pristine PPy. The C=C backbone stretching vibrations at 1580 cm^{-1} are moved to 1593 cm^{-1}, and the peaks at 1376, 1068, and 967 cm^{-1} corresponding to the bipolaron structure, observed in the spectrum of pristine PPy, are shifted, respectively, to 1381, 1080, and 978 cm^{-1} in the presence of the dye. This is connected to the interaction of PPy with the AF dye, as mentioned earlier in FTIR analysis.

The spectra of PPy with the dye exhibit an increase in the intensity of the band of C-H deformation in the bipolaron structure situated at 1080 cm^{-1} compared to the band at 1068 cm^{-1} in the pristine PPy. The intensity of the peak at 1080 cm^{-1} observed for the lowest dye concentration of 2.5 mM in PPy subsequently decreases upon further addition of the dye. As the bipolarons are dominant charge carriers in PPy, higher bipolaron content can be correlated with the higher conductivity of PPy.[29,36]

3.4. Yield and Conductivity. The yield is calculated with respect to the monomer used in the polymerization reaction. Theoretically, 1 g of pyrrole provides 1.23 g of PPy chloride (**Figure 1a**).

Herein, we observe that the yield in the synthesis of globular PPy is lower, which, however, increases with the use of the dye and thus shows the incorporation of the dye **(Table 1)**.

Table 1. Yield and Conductivity of the PPy Prepared at Different Molar Concentrations of AF with a Fixed Molar Ratio of the Oxidant to Pyrrole, i.e., [Oxidant]/[Pyrrole] = 2

[AF] (mM)	yield (g g^{-1})	conductivity (S cm^{-1})
0	0.90	1.1 ± 0.2
2.5	1.54	14.7 ± 0.5
7.5	1.62	8.2 ± 0.3
10.0	1.46	5.3 ± 0.3

Globular PPy possesses a conductivity of 1.1 S cm^{-1} **(Table 1)**, which is in good agreement with previously published results.[37] As presented in **Table 1**, the conductivity of PPy increases up to 14.7 S cm^{-1} for the PPy nanofibers prepared in the presence of 2.5 mM AF dye. The increase in the conductivity can be attributed to the higher content of charge carriers, bipolarons, in the nanofibrillar PPy, as evidenced by Raman spectroscopy **(see Section 3.3)**. It can be observed that the further increase in the dye concentration lowers the conductivity; however, it is still greater in all cases compared to globular PPy. As visible in SEM **(Figure 2d)** and TEM **(Figure 3d)** images, increase in the dye concentration to 10 mM invokes the formation of dye aggregates (nonconducting islands) on the surface of nanofibers, leading to the inhomogeneity of the material; as a result, a decrease in the conductivity was observed, and hence, the further increase in dye concentration was not studied. It is previously well reported that the conductivity of globular PPy can increase up to 2 orders of magnitude[22,23] when organic dyes are added to the preparation procedure, depending on the nanostructure obtained.

3.5. Thermal Studies. TGA was carried out to study the thermal stability of globular and nanofibrous PPy (**Figure 6).**

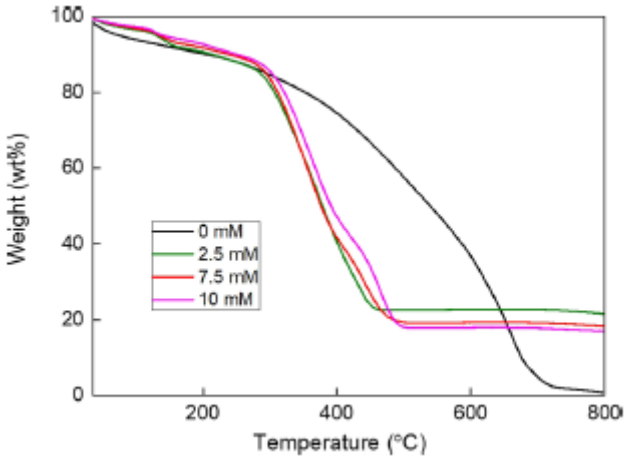

Figure 6. TGA of PPy prepared with different AF concentrations.

In all the cases, PPy shows stability up to nearly 200 °C, whereas a small weight loss is observed, which might be due to the removal of moisture. The thermal stability of PPy composites with the dye is higher

than that of the pristine PPy. PPy nanofibers leave a residue of ~20 wt % as compared to globular PPy with no residual weight.

3.6. Electrochemical Studies. In order to examine the potential in electrochemical capacitors, CV was performed for the prepared PPy, without and with the AF dye. **Figure 7** presents the CV, carried out by the drop-casting method as explained above in the Experimental Section. Different scan rates of 10, 20, 50, 100, and 200 mV s^{-1} were used over the potential range from -0.35 to 0.75 V in 0.2 M HCl.

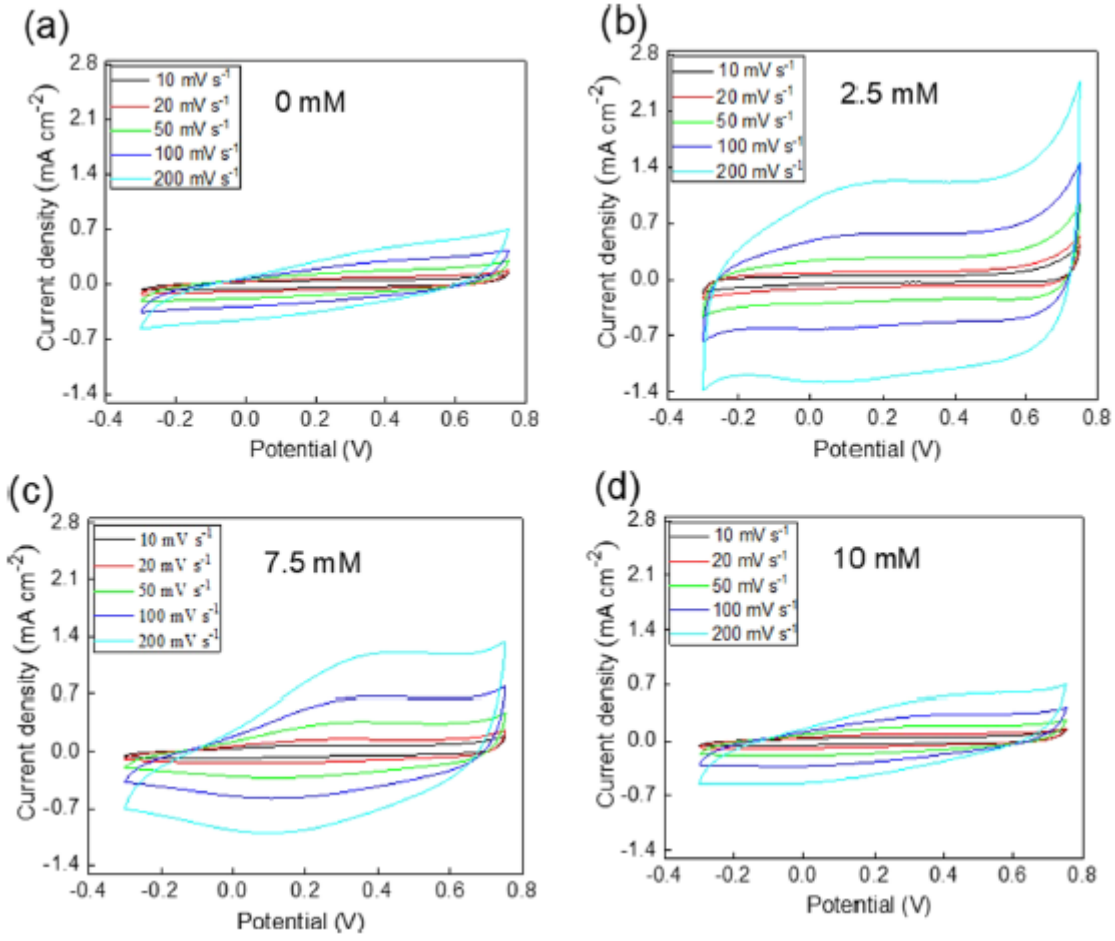

Figure 7. Cyclic voltammograms of PPy prepared in the presence of (a) 0, (b) 2.5, (c) 7.5, and (d) 10 mM AF.

Globular PPy shows oxidation and reduction peaks **(Figure 7a)** similar to previously reported studies.[38,39] The cyclic voltammograms evidently display the influence of the dye on the current densities of PPy, which further affect their redox behavior. Herein, for the lowest dye concentration of 2.5 mM, a sudden increase in the current density was observed, resulting in an enhanced redox peak and provided with a quasi-rectangular shaped curve, thus signifying better capacitive properties. For higher dye concentrations, 7.5 or 10 mM **(Figure 7c,d)**, however, a gradual decrease in the redox behavior, still better or similar to PPy alone, was observed, respectively. These cyclic voltammograms were further studied to evaluate the gravimetric capacitances based on their integral areas, as presented in **Table 2.** PPy itself is believed to have good capacitive behavior. The highest gravimetric capacitance was observed for the lowest dye concentration, which is fairly stable even at high potential scan rates. The enhanced capacitive behavior is also in accordance with the highest conductivity value

obtained **(Table 2)**. However, for other dye concentrations, lower capacitances which decay upon increasing the sweep rates, one of the commonly seen behaviors, were observed. It can be summarized that the presence of a AF certainly increases the capacitive property of PPy with the maximum capacitance of 85 F g^{-1} for the lowest amount of the dye.

Table 2. Gravimetric Capacitances (F g) of PPy with Different AF Concentrations at Various Scan Rates

	gravimetric capacitances (F g^{-1})			
	concentration of the dye			
scan rates (mV s^{-1})	0 mM	2.5 mM	7.5 mM	10 mM
10	62.1	85.6	78.2	60.3
20	47.5	78.4	70.1	47.3
50	35.7	76.2	61.7	38.2
100	28.2	74.9	54.7	32.0
200	22.2	75.2	47.4	26.3

3.7. Antibacterial Properties. The assessment of antimicrobial activity is commonly achieved either by the diffusion or by the dilution method. In the dilution method, the minimum concentration of the antibacterial material to inhibit the bacterial growth, in media such as agar or broth, is determined, termed as MIC, which is often expressed in mg mL^{-1} or ,µg mL^{-1}.[40] In the current study, the MIC was determined by the CLSI/EUCAST macrodilution method for the prepared PPy-containing AF dye. The PPy nanofibers show abrupt rise in the antibacterial activity against both bacteria, irrespective of the dye concentrations, as presented in **Table 3**. The antibacterial activity of PPy can be related to various effects which have been previously described by Silva junior et al.[41]

Table 3. Results of the MIC of the PPy in the Presence of (a) 0, (b) 2.5, (c) 7.5, and (d) 10 mM AF

	minimal inhibitory concentration (mg mL^{-1})			
bacteria	0 mM	2.5 mM	7.5 mM	10 mM
S. aureus	16	2	2	4
E. coli	16	4	4	4

The dye concentrations, 2.5 and 7.5 mM, show similar decreased MIC values of 2 and 4 mg mL^{-1} against *S. aureus* and *E. coli*, respectively, compared to PPy alone, signifying the enhanced antibacterial activity with incorporation of the dye. However, for the highest concentration, the response of the Gram-positive bacterium is reduced as the MIC value is increased to 4 mg mL^{-1}, but against the Gram-negative bacterium, no changes were observed.

In recent years, the antibacterial activity of PPy has gained significant interest. For example, Salabat et al. demonstrated the influence of palladium on the antibacterial activity of PPy against *S. aureus* by the microdilution method and obtained an MIC of 5.78 mg mL^{-1}.[12] Using the broth dilution method, Maruthapandi et al. presented the effect of Zn/CuO on the antibacterial activity of PPy with an MIC of 1 mg mL^{-1}.[13] It is clear that PPy has lower antibacterial activity; however, it can be improved with the addition of a variety of metal or metal oxides; nevertheless, the complicated synthesis and high cost are the major disadvantages. Herein, with the support of an inexpensive organic dye, we have

successfully enhanced the antibacterial effect against the two bacteria with the lowest MIC of 2 mg mL^{-1}.

4. CONCLUSIONS

The successful preparation of PPy nanofibers in the presence of the AF dye, using iron(III) chloride was achieved. A maximum conductivity of 14.7 S cm^{-1} for PPy with the lowest dye concentration was observed. The FTIR and Raman spectroscopy confirmed the structure of PPy and its interaction with the AF dye. The higher bipolaron fraction in the PPy-containing dye was also indicated through Raman spectroscopy at a 633 nm excitation. The highest gravimetric capacitance of 85 F g^{-1} was observed for PPy prepared with the 2.5 mM dye at a scan rate of 10 mV s^{-1}. Additionally, the PPy-containing AF dye demonstrated enhanced antibacterial activity against both *S. aureus* and *E. coli* bacteria. Therefore, the addition of AF during PPy synthesis offers improved materials with possible applications in biosensors, antimicrobial surfaces, and bioelectronic devices. The low cost and easy availability of an organic dye are additional advantages in making the overall process simple and cost-effective.

REFERENCES

(1) Gerard, M.; Chaubey, A.; Malhotra, B. D. Application of conducting polymers to biosensors. Biosens. Bioelectron. 2002, 17, 345-359.

(2) Snook, G. A.; Kao, P.; Best, A. S. Conducting-polymer-based supercapacitor devices and electrodes. J. Power Sources 2011, 196, 112.

(3) Humpolíček, P.; Kašpárková, V.; Pacherník, J.; Stejskal, J.; Bober, P.; Capáková, Z.; Radazkiewicz, K. A.; Junkar, I.; Lehocky, M. The biocompatibility of polyaniline and polypyrrole: A comparative study of their cytotoxicity, embryotoxicity and impurity profile. Mater. Sci. Eng., C 2018, 91, 303-310.

(4) Mahat, M. M.; Sabere, A. S. M.; Azizi, J.; Amdan, N. A. N. Potential Applications of Conducting Polymers to Reduce Secondary Bacterial Infections among COVID-19 Patients: a Review. Emergent Mater. 2021, 4, 279-292.

(5) Maráková, N.; Humpolíček, P.; Kašpárková, V.; Capáková, Z.; Martinková, L.; Bober, P.; Trchová, M.; Stejskal, J. Antimicrobial activity and cytotoxicity of cotton fabric coated with conducting polymers, polyaniline or polypyrrole, and with deposited silver nanoparticles. Appl. Surf. Sci. 2017, 396, 169-176.

(6) Liu, J.; Wang, J.; Yu, X.; Li, L.; Shang, S. One-pot synthesis of polypyrrole/AgCl composite nanotubes and their antibacterial properties. Micro & Nano Lett. 2015, 10, 50-53.

(7) Bideau, B.; Bras, J.; Saini, S.; Daneault, C.; Loranger, E. Mechanical and antibacterial properties of a nanocellulose-polypyrrole multilayer composite. Mater. Sci. Eng., C 2016, 69, 977-984.

(8) Nazarzadeh Zare, E.; Mansour Lakouraj, M.; Mohseni, M. Biodegradable polypyrrole/dextrin conductive nanocomposite: synthesis, characterization, antioxidant and antibacterial activity. Synth. Met. 2014, 187, 9-16.

(9) Ahmad, N.; Sultana, S.; Faisal, S. M.; Ahmed, A.; Sabir, S.; Khan, M. Z. Zinc oxide-decorated polypyrrole/chitosan bionanocomposites with enhanced photocatalytic, antibacterial and anticancer performance. RSC Adv. 2019, 9, 41135-41150.

(10) Milakin, K. A.; Capáková, Z.; Acharya, U.; Vajdák, J.; Morávková, Z.; Hodan, J.; Humpolícek, P.; Bober, P. Biocompatible and antibacterial gelatin-based polypyrrole cryogels. Polymer 2020, 197, 122491:1-7.

(11) Xu, Y.; Ma, J.; Han, Y.; Xu, H.; Wang, Y.; Qi, D.; Wang, W. A simple and universal strategy to deposit Ag/polypyrrole on various substrates for enhanced interfacial solar evaporation and antibacterial activity. Chem. Eng. J. 2020, 384, 123379:1-9.

(12) Salabat, A.; Mirhoseini, F.; Mahdieh, M.; Saydi, H. A novel nanotube-shaped polypyrrole-Pd composite prepared using reverse microemulsion polymerization and its evaluation as an antibacterial agent. New J. Chem. 2015, 39, 4109-4114.

(13) Maruthapandi, M.; Sharma, K.; Luong, J. H. T.; Gedanken, A. Antibacterial activities of microwave-assisted synthesized polypyrrole/chitosan and poly (pyrrole-N-(l-naphthyl) ethylenediamine) stimulated by C-dots. Carbohydr. Polym. 2020, 243, 116474.

(14) Zasońska, B. A.; Acharya, U.; Pfleger, J.; Humpolícek, P.; Vajdák, J.; Svoboda, J.; Petrovsky, E.; Hromádková, J.; Walterova, Z.; Bober, P. Multifunctional polypyrrole@ maghemite@ silver composites: synthesis, physico-chemical characterization and antibacterial properties. Chem. Pap. 2018, 72, 1789-1797.

(15) Bober, P.; Liu, J.; Mikkonen, K. S.; Ihalainen, P.; Pesonen, M.; Plumed-Ferrer, C.; von Wright, A.; Lindfors, T.; Xu, C.; Latonen, R.-M. Biocomposites of nanofibrillated cellulose, polypyrrole, and silver nanoparticles with electroconductive and antimicrobial properties. Biomacromolecules 2014, 15, 3655-3663.

(16) Wu, T.-M.; Chang, H.-L.; Lin, Y.-W. Synthesis and characterization of conductive polypyrrole/multi-walled carbon nanotubes composites with improved solubility and conductivity. Compos. Sci. Technol. 2009, 69, 639-644.

(17) Hsu, F.-H.; Wu, T.-M. In situ synthesis and characterization of conductive polypyrrole/graphene composites with improved solubility and conductivity. Synth. Met. 2012, 162, 682-687.

(18) Bose, S.; Kuila, T.; Uddin, M. E.; Kim, N. H.; Lau, A. K. T.; Lee, J. H. In-situ synthesis and characterization of electrically conductive polypyrrole/graphene nanocomposites. Polymer 2010, 51, 5921-5928.

(19) Jurewicz, K.; Delpeux, S.; Bertagna, V.; Béguin, F.; Frackowiak, E. Supercapacitors from nanotubes/polypyrrole composites. Chem. Phys. Lett. 2001, 347, 36-40.

(20) Biswas, S.; Drzal, L. T. Multilayered nanoarchitecture of graphene nanosheets and polypyrrole nanowires for high performance supercapacitor electrodes. Chem. Mater. 2010, 22, 5667-5671.

(21) Li, Y.; Bober, P.; Trchová, M.; Stejskal, J. Polypyrrole prepared in the presence of methyl orange and ethyl orange: nanotubes versus globules in conductivity enhancement. J. Mater. Chem. C 2017, 5, 4236-4245.

(22) Minisy, I. M.; Bober, P.; Acharya, U.; Trchová, M.; Hromádková, J.; Pfleger, J.; Stejskal, J. Cationic dyes as morphology-guiding agents for one-dimensional polypyrrole with improved conductivity. Polymer 2019, 174, 11-17.

(23) Minisy, I. M.; Bober, P.; Šeděnková, I.; Stejskal, J. Methyl red dye in the tuning of polypyrrole conductivity. Polymer 2020, 207, 122854:1-9.

(24) Bober, P.; Li, Y.; Acharya, U.; Panthi, Y.; Pfleger, J.; Humpolícek, P.; Trchová, M.; Stejskal, J. Acid Blue dyes in polypyrrole synthesis: the control of polymer morphology at nanoscale in the promotion of high conductivity and the reduction of cytotoxicity. Synth. Met. 2018, 237, 40-49.

(25) Dana, S.; Prusty, D.; Dhayal, D.; Gupta, M. K.; Dar, A.; Sen, S.; Mukhopadhyay, P.; Adak, T.; Dhar, S. K. Potent antimalarial activity of acriflavine in vitro and in vivo. ACS Chem. Biol. 2014, 9, 23662373.

(26) Lee, K.; Zhang, H.; Qian, D. Z.; Rey, S.; Liu, J. O.; Semenza, G. L. Acriflavine inhibits HIF-1 dimerization, tumor growth, and vascularization. Proc. Natl. Acad. Sci U.S.A. 2009, 106, 17910-17915.

(27) Wiegand, I.; Hilpert, K.; Hancock, R. E. W. Agar and broth dilution methods to determine the minimal inhibitory concentration (MIC) of antimicrobial substances. Nat. Protoc. 2008, 3, 163-175.

(28) Marjanovic, B.; Ciric-Marjanovic, G.; Radulovic, A.; Juranic, I.; Holler, P. Synthesis and characterization of polyacriflavine. Mater. Sci. Forum 2007, 555, 503-508.

(29) Stejskal, J.; Trchová, M.; Bober, P.; Morávková, Z.; Kopecky, D.; Vrnata, M.; Prokes, J.; Varga, M.; Watzlová, E. Polypyrrole salts and bases: superior conductivity of nanotubes and their stability towards the loss of conductivity by deprotonation. RSC Adv. 2016, 6, 88382-88391.

(30) Crowley, K.; Cassidy, J. In situ resonance Raman spectroelec-trochemistry of polypyrrole doped with dodecylbenzenesulfonate. J. Electroanal. Chem. 2003, 547, 75-82.

(31) Gupta, S. Hydrogen bubble-assisted syntheses of polypyrrole micro/nanostructures using electrochemistry: structural and physical property characterization. J. Raman Spectrosc. 2008, 39, 1343-1355.

(32) Morávková, Z.; Taboubi, O.; Minisy, I. M.; Bober, P. The evolution of the molecular structure of polypyrrole during chemical polymerization. Synth. Met. 2021, 271, 116608:1-6.

(33) Minisy, I. M.; Acharya, U.; Kobera, L.; Trchová, M.; Unterweger, C.; Breitenbach, S.; Brus, J.; Pfleger, J.; Stejskal, J.; Bober, P. Highly conducting 1-D polypyrrole prepared in the presence of safTanin. J. Mater. Chem. C 2020, 8, 12140-12147.

(34) Ishpal; Kaur, A. Spectroscopic and electrical sensing mechanism in oxidant-mediated polypyrrole nanofibers/nanoparticles for ammonia gas. J. Nanopart. Res. 2013, 15, 1637:1-14.

(35) Liu, Y.-C. Characteristics of vibration modes of polypyrrole on surface-enhanced Raman scattering spectra. J. Electroanal. Chem. 2004, 571, 255-264.

(36) Varga, M.; Kopecká, J.; Morávková, Z.; Krivka, I.; Trchová, M.; Stejskal, J.; Prokes, J. Effect of oxidant on electronic transport in polypyrrole nanotubes synthesized in the presence of methyl orange. J. Polym. Sci., PartB: Polym. Phys. 2015, 53, 1147-1159.

(37) Acharya, U.; Bober, P.; Trchová, M.; Zhigunov, A.; Stejskal, J.; Pfleger, J. Synergistic conductivity increase in polypyrrole/molybde-num disulfide composite. Polymer 2018, 150, 130-137.

(38) Fan, X.; Yang, Z.; He, N. Hierarchical nanostructured polypyrrole/graphene composites as supercapacitor electrode. RSC Adv. 2015, 5, 15096-15102.

(39) Liu, Y.; Wang, H.; Zhou, J.; Bian, L.; Zhu, E.; Hai, J.; Tang, J.; Tang, W. Graphene/polypyrrole intercalating nanocomposites as supercapacitors electrode. Electrochim. Acta 2013, 112, 44-52.

(40) Balouiri, M.; Sadiki, M.; Ibnsouda, S. K. Methods for in vitro evaluating antimicrobial activity: A review. J. Pharm. Anal. 2016, 6, 71-79.

(41) Silva Junior, F. A. G. d.; Vieira, S. A.; Botton, S. D. A.; Costa, M. M. D.; Oliveira, H. P. D. Antibacterial activity of polypyrrole-based nanocomposites: a mini-review. Polimeros 2020, 30, No. E2020048:1-9.